

# Spectroscopic Analysis of Poly (Methacrylic Acid-co-Ethylene Glycol Dimethacrylate) Submicron Particles by Fluorescence Emission and Light Scattering upon Binding with 17 $\beta$ -Estradiol in Water Treatment

Yu Yang<sup>1</sup>, Edward P.C. Lai<sup>1,\*</sup> and Min Liu<sup>2</sup>

<sup>1</sup>Department of Chemistry, Ottawa-Carleton Chemistry Institute, Carleton University, 1125 Colonel By Drive, Ottawa, Ontario K1S 5B6, Canada

<sup>2</sup>Department of Chemistry, Huazhong University of Science and Technology, Wuhan, Hubei, 430074, P.R. China

**Abstract:** An investigation of light scattering of non-imprinted poly methacrylic acid-co-ethylene glycol dimethacrylate (PMAA-co-EGDMA) submicron particles (300 $\pm$ 5 nm) in aqueous suspension before and after 17 $\beta$ -estradiol (E2) binding was conducted by using a spectrofluorimeter. An optimal excitation wavelength to determine Mie scattering from these submicron particles was 725 $\pm$ 1 nm for the highest intensity. This light scattering from non-imprinted polymer (NIP) submicron particles in aqueous suspension was increased by spiking E2 at various concentrations (from 0.1 to 1.0 ppm). Thus, a new alternative method was found to determine E2 in a water sample by measurement of light scattering from NIP particles using spectrofluorimetry. Furthermore, the light scattering at 725 nm from E2 solution was increased by spiking NIP particles at various concentrations (from 0.02 to 0.12 ppm) but the fluorescence emission essentially stayed constant. The fluorescence emission from E2, however, increased more significantly in the presence of NIP particles than E2 spiking into water alone.

**Keywords:** Light scattering, fluorescence emission, 17 $\beta$ -estradiol, poly (MAA-co-EGDMA), submicron particles.

## 1. INTRODUCTION

Molecularly imprinted polymer (MIP) and non-imprinted polymer (NIP) particles of all sizes have been adopted for cleanup or preconcentration of environmental pollutants [1]. The advantages of using these functional polymers are excellent efficiency on capture of organic pollutants at trace concentration levels, and cost effectiveness, allowing for the fast processing of wastewater effluent in large volumes or at high flow rates [2]. The polymers are synthesized from monomers bearing functional groups (or functional monomers), such as methacrylic acid (MAA), acrylic acid (AA), pyrrole (Py), 4-vinylpyridine (4-VP), and 3-(2-aminoethylamino) propyl-trimethoxysilane (APTMS) [2-6]. The most commonly used cross-linkers in MIP and NIP synthesis are EDMA, EGDMA, TRIM, PETRA, TEOS and DVB [2, 7-11]. An ultra-high specific surface area is a major characteristic of the three dimensional (3-D) cross-linked structure that has become especially important to the development of MIP and NIP submicron particles [12].

Endocrine disrupting contaminants (EDCs) have a significant impact on ecological systems in the global environment [13-15]. Due to their ability to disrupt the central regulatory functions in humans [16], EDCs have been seen as highly carcinogenic, especially causing breast cancer and

human infertility [17]. Among EDCs, estrogenic compounds are mainly natural steroids and synthetic compounds with biological metabolisms. Estrone (E1), 17 $\beta$ -estradiol (E2), 17 $\alpha$ -ethinylestradiol (EE2) and bisphenol A (BPA) are among the most potent estrogenic compounds found in environmental water sources. Their chemical structures can be seen in Fig. (1).

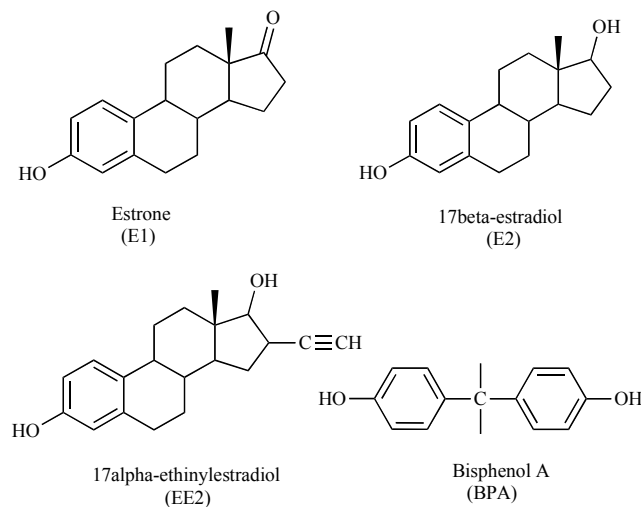


Fig. (1). Molecular structures of estrogenic compounds.

Selective removal of one model estrogenic compound, E2, by using functional MIPs and NIPs has been investigated by several research groups [18-21]. The binding between functional MIPs and E2 involves non-covalent molecular

\*Address correspondence to this author at the Department of Chemistry, Ottawa-Carleton Chemistry Institute, Carleton University, 1125 Colonel By Drive, Ottawa, Ontario K1S 5B6, Canada; Tel: 613 520 2600 ext; 3835 Fax: 613 520 3749; E-mail: edward\_lai@carleton.ca

interaction [7] via H-bonding between the carboxyl groups specifically arranged in templated cavities and hydroxyl groups in the E2 molecule. The binding of NIPs with E2 molecule is envisaged as non-specific interaction of its hydroxyl groups with independent carboxyl groups distributed throughout the 3-D structure [5].

In the present study, we have used poly (MAA-co-EGDMA) particles to non-covalently bind with E2. As the E2 molecules randomly bound on the surface of NIP particles (in aqueous suspension), an opportunity to preconcentrate them together becomes available. Is the signal coming from free E2 molecules in the sample solution, or from E2 molecules bound on NIP particles in aqueous suspension? Our careful investigation of this challenging issue is reported in details below.

## 2. EXPERIMENTAL

### 2.1. Chemicals and Reagents

17 $\beta$ -Estradiol and bisphenol A were purchased from Sigma-Aldrich (St. Louis, MO, USA). HPLC grade methanol was purchased from Caledon (Georgetown, ON, Canada). 18-M $\Omega$ .cm distilled deionized water (DDW) was obtained from a Millipore Milli-Q water system (Bedford, MD, USA). The procedure for synthesis of polymethacrylic acid (PMAA) non-imprinted polymer (NIP) submicron particles was based on a previously established method, in the absence of any template molecule [22]. A stock E2 solution was prepared in HPLC grade methanol at a concentration of 1000 ppm. A stock aqueous suspension of PMAA NIP submicron particles was prepared in DDW at a concentration of 20 ppm. All aqueous suspensions of NIP particles were treated by an ultrasonic system (Branson 2510, Danbury, CT, USA) for 10 min before use.

### 2.2. Determination of the Optimal Mie Scattering Excitation Wavelength for PMAA NIP Submicron Particles in Aqueous Suspension

Mie scattering spectra of 0.5 ppm NIP particles in aqueous suspension was measured by a fluorescence spectrophotometer (Varian Cary Eclipse, Palo Alto, CA, USA) using excitation wavelengths in the range from 200 $\pm$ 1 nm to 750 $\pm$ 1 nm, with both excitation and emission slits equal to 5 nm.

### 2.3. Determination of Light Scattering and Fluorescence Emission Intensities of Various Concentrations of E2 Spiked Into Aqueous Suspension of NIP Submicron Particles

2.0  $\mu$ L of 100 ppm E2 methanol solution was added into a quartz cuvette which contained 2.0 mL of 0.1 ppm NIP particles in aqueous suspension. The light scattering and fluorescence emission spectra of this mixture, after thorough shaking, was measured at excitation wavelengths of 700 $\pm$ 1 nm, 725 $\pm$ 1 nm and 750 $\pm$ 1 nm to obtain three light scattering spectra, and at 279 $\pm$ 1 nm to obtain one fluorescence emission spectrum. Another nine measurements were performed similarly by adding 4.0-20  $\mu$ L of 100 ppm E2 methanol solution. Similarly, light scattering spectra were acquired for a mixture of 0.1 ppm NIP particles and 0.5 ppm BPA.

### 2.4. Determination of Light Scattering and Fluorescence Emission Intensities of Various Concentrations of PMAA NIP Submicron Particles in Aqueous Suspensions Spiked with E2 Using Excitation Wavelengths of 279 $\pm$ 1 nm and 725 $\pm$ 1 nm

2.0  $\mu$ L of 20 ppm stock NIP particles in aqueous suspension was transferred into a quartz cuvette which contained 2.0 mL of 1.0 ppm E2 aqueous solution. The light scattering and fluorescence emission spectra of this mixture, after thorough shaking, were measured using excitation wavelengths of 279 $\pm$ 1 nm and 725 $\pm$ 1 nm. Another five measurements were performed similarly by transferring 4.0-12.0  $\mu$ L of 20 ppm stock NIP particles in aqueous suspension.

### 2.5. FTIR Analysis

All infrared spectra were measured using a Varian 1000 Scimitar Series FTIR spectrometer with Varian resolutions software. Samples were prepared by pressing 1.7-2.0 mg of solid sample and 100 mg of dehydrated KBr in a die to make transparent pellets.

## 3. RESULTS AND DISCUSSION

### 3.1. Optimal Mie Scattering Wavelength for PMAA-co-EGDMA NIP Submicron Particles in Aqueous Suspension

Two types of light scattering are usually observed in spectroscopic analysis of a sample solution containing organic compounds. One type is Rayleigh scattering, which has the same wavelength as the incident light [23]. The other type is Raman scattering which appears at longer wavelengths than the incident light [24]. In addition, Mie scattering can show up on top of Rayleigh scattering if the solution contains suspending particles.

Mie scattering is a perfect method to measure light scattering from spherical submicron particles. The peak intensity can be used to determine the concentration of NIP particles in aqueous suspension [25]. The best excitation wavelength for Mie scattering from NIP particles need to be found in our research. Fig. (2) shows that Mie scattering of visible light by NIP submicron particles in aqueous suspension was observed as sharp spectral peaks. All the Mie scattering peaks had the same wavelengths as the incident lights. From 700 $\pm$ 1 nm to 750 $\pm$ 1 nm, this wavelength range exhibited the most intense Mie scattering (725 $\pm$ 1 nm > 700 $\pm$ 1 nm > 720 $\pm$ 1 nm > 730 $\pm$ 1 nm > 710 $\pm$ 1 nm > 740 $\pm$ 1 nm  $\approx$  750 $\pm$ 1 nm) than all lower wavelengths. The best wavelength for strong Mie scattering from the NIP particles was 725 $\pm$ 1 nm which gave the highest intensity of 783 $\pm$ 1 arbitrary units (a.u.). It would provide optimal sensitivity for determining the concentration of NIP particles in aqueous suspension. One plausible explanation for this best wavelength is the size of submicron particles. Another factor is incident light intensity from the spectrofluorometer and spectral response of its detector, which can vary with the excitation wavelength setting. Note that Mie scattering has the highest intensity at a detection angle of 180 degrees with respect to the incident light [26]. Using a spectrofluorimeter to measure the Mie scattering from NIP submicron particles permits only the detection of scattering light at 90 degrees to the incident light. Therefore,

the most intense Mie scattering from NIP submicron particles was not recorded by the spectrofluorimeter.

### 3.2. Light Scattering from NIP Particles in Aqueous Suspension Upon Binding with E2

The best excitation wavelength to determine Mie scattering from our NIP submicron particles in aqueous suspension using the spectrofluorimeter was  $725 \pm 1$  nm. The wavelength range from 700 nm to 750 nm provided nearly optimal results for Mie scattering. Next, the effect on light scattering after E2 addition into the NIP particles was further investigated. Fig. (3) shows the light scattering spectra of 0.1-ppm NIP particles in aqueous suspension, before and after binding with E2 in the concentration range from 0.1 ppm to 1.0 ppm. At all three wavelengths of incident light, the scattering peak intensities were distinctly increased by E2 addition. For instance, the peak intensity observed after binding with 0.3-

ppm E2 was higher than those with 0.2, 0.1 and 0.0-ppm E2. Note that the wavelengths  $725 \pm 1$  nm and  $750 \pm 1$  nm exhibited irregularity in peak intensities upon binding with 1.0-ppm E2. Even though the enhancement of light scattering from NIP particles due to E2 binding was of unknown nature until further investigation, its significance could be three-fold. First, the peak intensity was no longer determined by the concentration of NIP particles only. Second, the increase in peak intensity provided a new analytical parameter for the determination of E2 down to 0.1 ppm or lower. Third, it would not be straightforward any more to determine, by light scattering measurement, the amount of NIP particles that could pass through a syringe filter (after a binding experiment with E2).

In the standard calibration curves of light scattering intensities versus concentration of E2 added to 0.1-ppm NIP particles in aqueous suspension. The  $700 \pm 1$  nm wavelength

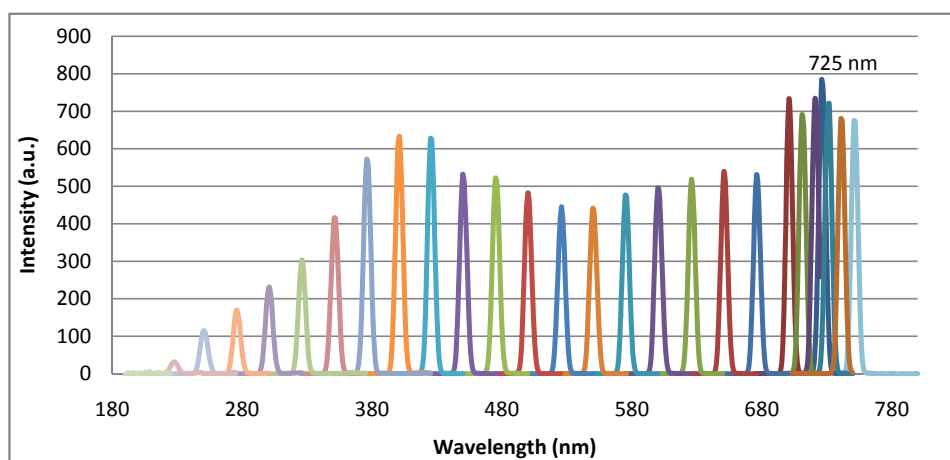


Fig. (2). Mie scattering spectra of 0.5-ppm NIP particles in aqueous suspension, by scanning the incident light from  $750 \pm 1$  nm to  $200 \pm 1$  nm.

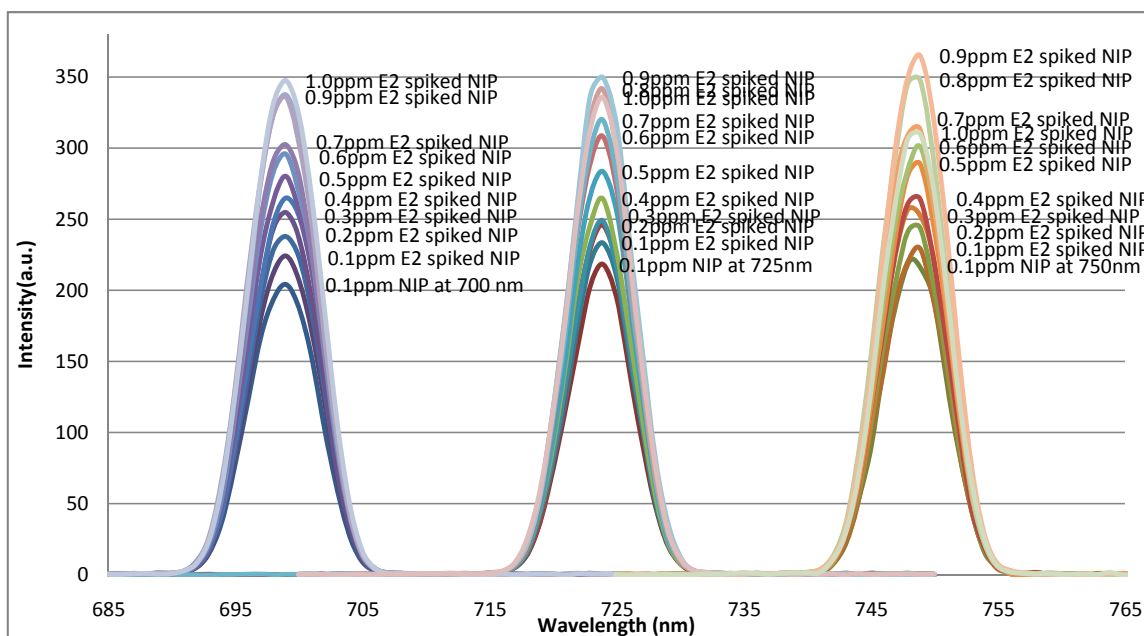


Fig. (3). Light scattering spectra from 0.1-ppm NIP particles in aqueous suspension upon binding with E2 (from 0.1 ppm to 1.0 ppm), by scanning the incident light around 700 nm, 725 nm and 750 nm.

gave the best correlation coefficient of 0.9862. The sensitivity of light scattering measurement, based on the slope of each calibration curve, increased from 132.6 a.u./ppm at  $700\pm 1$  nm to 160.7 a.u./ppm at  $750\pm 1$  nm. Thus, measuring the light scattering intensity is a new alternative method that can be used to determine the concentration of E2 (down to 0.1 ppm or less) in unknown samples. This method would be valuable especially for organic compounds which do not exhibit strong molecular fluorescence or UV-visible absorbance. In Fig. (4), a non-fluorescent organic compound, bisphenol A (BPA), was successfully observed to exhibit enhancement in light scattering from the NIP particles after binding BPA and NIP particles together. Fluorescence analysis of 35-ppm BPA using excitation wavelengths of 190, 200, 250, 280, 300, 350 and 400 nm did not detect any emission intensity in the wavelength range from 190-800 nm.

Now, using this new method, BPA was detectable at 0.5 ppm with good sensitivity. The only requirement to determine these target molecules is addition of 0.1-ppm NIP particles to all unknown samples and standard solutions. It is probably the sharp profile of the light scattering peak (with a full width at half maximum of  $7.9\pm 0.1$  nm) that renders this method much more sensitive than conventional UV-visible spectrophotometry.

### 3.3. Comparison of Fluorescence Emissions from E2 Added to NIP Particles in Aqueous Suspension and E2 in Aqueous Solution

After E2 was found to significantly enhance the light scattering by NIP particles in aqueous suspension, the reverse effect of NIP particles on E2 fluorescence emission was investigated. Fig. (5) shows the fluorescence emission

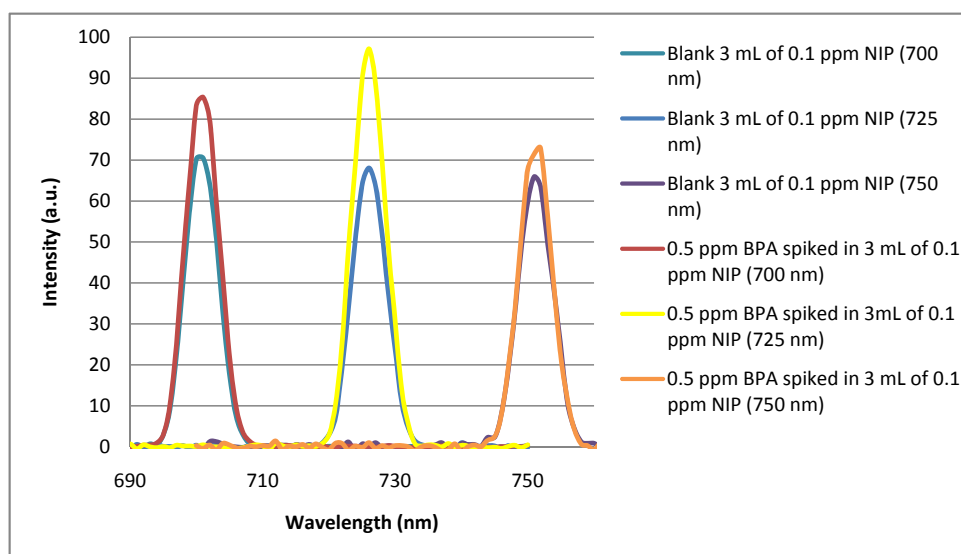


**Fig. (4).** Light scattering spectra from 0.1-ppm NIP particles in aqueous suspension upon binding with bisphenol A (0.5 ppm), by scanning the incident light around 700 nm, 725 nm and 750 nm.

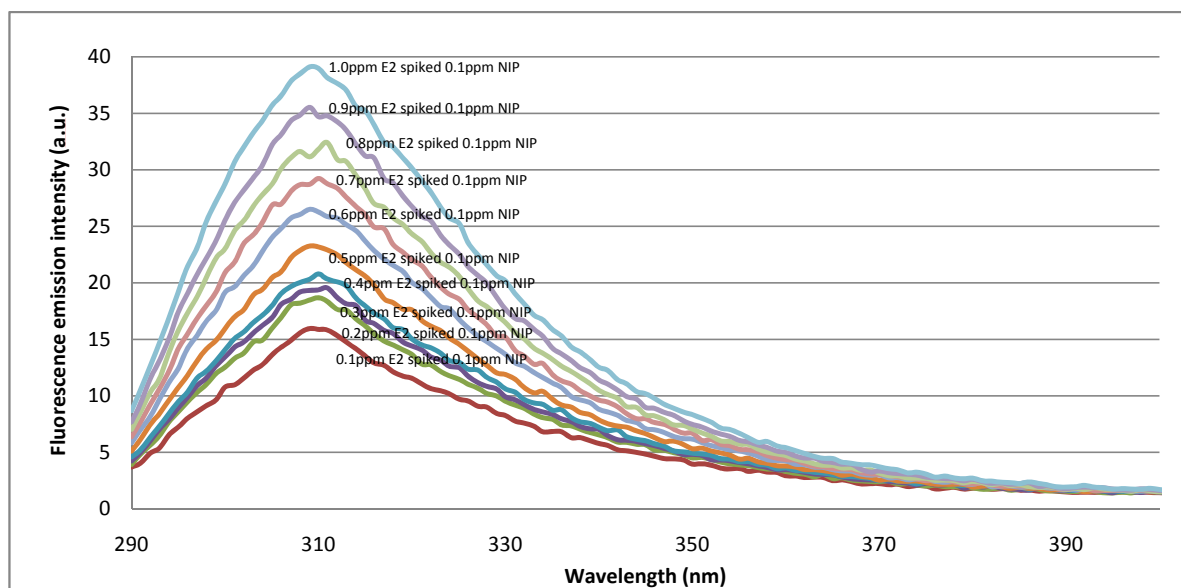


**Fig. (5).** Fluorescence emission spectra of 0.1 to 1.0-ppm E2 added to 0.1-ppm NIP particles in aqueous suspension, using excitation wavelength =  $279\pm 1$  nm.

spectra of E2 added in various concentrations to 0.1-ppm NIP particles in aqueous suspension, using a fluorescence excitation wavelength of  $279\pm 1$  nm. The fluorescence emission intensity at  $310\pm 2$  nm increased successively when the concentration of E2 was raised from 0.1 ppm to 1.0 ppm. A standard calibration curve was constructed to verify a high correlation coefficient of 0.9824 and a sensitivity slope of  $25.3\pm 0.1$  a.u./ppm E2.

Fig. (6) shows the fluorescence emission spectra of E2 added in various concentrations to distilled deionized water (DDW), using a fluorescence excitation wavelength of  $279\pm 1$  nm, without any NIP particles. Similarly to Fig. (5), the fluorescence emission intensity at  $310\pm 2$  nm increased with higher concentration of E2. A standard calibration curve of fluorescence emission intensity vs. concentration of E2 added to DDW was constructed to indicate a higher correlation coefficient of 0.9907 and better sensitivity slope

of  $29.8\pm 0.1$  a.u./ppm E2 (in comparison to  $25.3\pm 0.1$  a.u./ppm from 0.1- to 1.0-ppm E2 spiked 0.1-ppm NIP suspension). Such a decrease in sensitivity of  $\sim 15\%$  was attributed to the diminution of excitation light and attenuation of fluorescence emission by the presence of NIP particles in each sample. Note that the fluorescence emission intensities from various concentrations of E2 when added to NIP particles in aqueous suspension were larger than added to DDW merely due to a larger background (or blank).

Table 1 shows the net (or blank subtracted) fluorescence emission intensities of E2 added to either DDW or 0.1-ppm NIP submicron particles in aqueous suspension. For instance, the fluorescence emission intensity of 0.1-ppm E2 spiked DDW was  $3.60\pm 0.05$  a.u. while the fluorescence emission intensity of 0.1-ppm E2 spiked 0.1-ppm NIP submicron particles in aqueous suspension was  $3.58\pm 0.05$  a.u. Generally, the fluorescence emission intensities in water (the

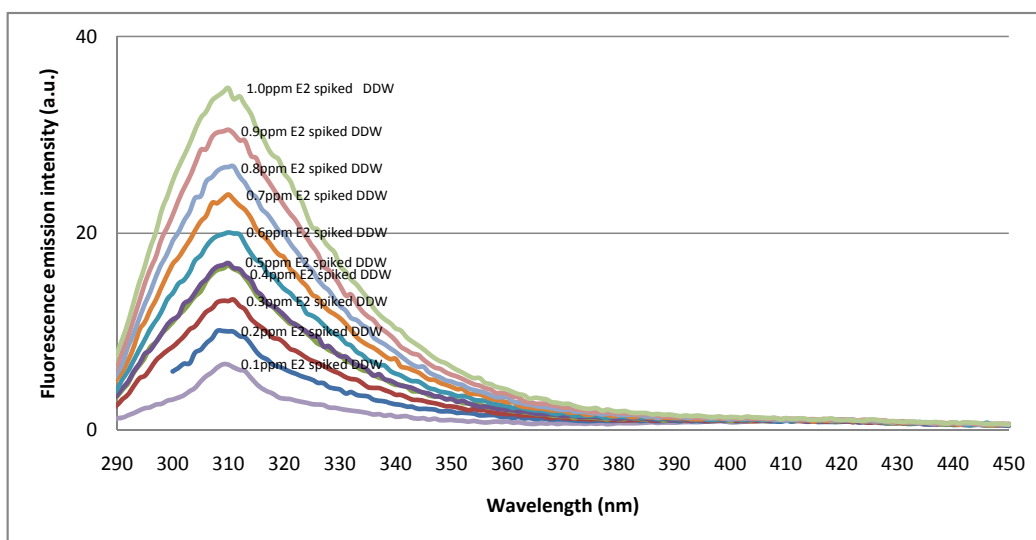


Fig. (6). Fluorescence emission spectra of 0.1 to 1.0-ppm E2 added to DDW, using excitation wavelength =  $279\pm 1$  nm.

Table 1. Net Fluorescence Intensities of E2 Spiked DDW and 0.1-ppm NIP Submicron Particles Aqueous Suspension

Concentration of E2 Spiked DDW (ppm)	Fluorescence Emission Intensity (Blank Subtracted) (a.u.)	Concentration of E2 (ppm) Spiked 0.1-ppm NIP	Fluorescence Emission Intensity (Blank Subtracted) (a.u.)
0.1	3.60	0.1	3.58
0.2	6.98	0.2	6.30
0.3	10.16	0.3	7.18
0.4	13.62	0.4	8.41
0.5	13.88	0.5	10.88
0.6	16.99	0.6	14.13
0.7	20.84	0.7	16.85
0.8	23.69	0.8	20.03
0.9	27.42	0.9	23.15
1.0	31.65	1.0	26.73

second column) are higher than the fluorescence emission intensities of E2 spiked NIP particles in aqueous suspension (the fourth column). In other words, the NIP particles (0.1 ppm) distinctly decreased the fluorescence emission intensity of E2 by  $15\pm 1\%$  ( $= 1 - \text{ratio of slopes in the standard calibration curves}$ ) due to diminution of the excitation light and attenuation of the fluorescence emission. Nonetheless, this spectroscopic property (15% lower fluorescence emission intensity) of poly (MAA-co-EGDMA) sub-micron particles is acceptable, or tolerable, for environmental monitoring and remediation applications. Most importantly, they can bind E2 molecules on an impressively fast time scale of seconds (data not shown). After using NIP particles to remove trace E2 from a large volume of contaminated water, it would still be possible to estimate the total amount of E2 (bound on suspending NIP particles) by fluorescence emission measurement (albeit with an error of 15%). However, we found the increasing fluorescence emission from E2 spiked NIP particles.

### 3.4. Fluorescence Emission and Light Scattering from Various Concentrations of NIP in Aqueous Suspension at fixed E2 Concentration

The enhancement of light scattering from NIP particles due to E2 binding (as discussed in Section 3.2) was further investigated, by varying the concentration of NIP particles in aqueous suspension with a fixed E2 concentration. Fig. (7) shows their fluorescence emission and light scattering spectra obtained using two excitation wavelengths,  $279\pm 1$  nm and  $725\pm 1$  nm. The intensities of light scattering at both excitation wavelengths increased with each increment of NIP particles. Two standard calibration curves were constructed for both light scatterings, which showed a better correlation of  $0.96\pm 0.01$  for  $725\pm 1$  nm than  $0.89\pm 0.01$  for  $279\pm 1$  nm. The longer wavelength,  $725\pm 1$  nm, is obviously better for the determination of NIP particle concentrations by light scattering. Fig. (7) also shows that, when the concentration

of NIP particles increased, the fluorescence emission intensity from E2 stayed essentially constant. Whereas this constant fluorescence emission was totally expected, the enhancement of light scattering (as discussed in Section 3.2) became even more fascinating to comprehend because the light scattering intensity produced by 1.0 ppm E2 at excitation wavelength =  $725\pm 1$  nm was only 15-20 a.u. in the standard calibration curve.

### 3.5. Spectroscopic Characterization of NIP and E2 Bound NIP Submicron Particles

The interaction between NIP submicron particles and E2 was characterized by FTIR spectroscopy. In Fig. (8), spectrum (a) represents NIP submicron particles before E2 binding, spectrum (b) shows NIP submicron particles after binding with E2, spectrum (c) shows NIP submicron particles in mixture with E2 particles, and spectrum (d) shows E2 particles. These FTIR spectra show detail information on the interaction between the NIP submicron particles and E2 molecules *via* H-bonding. In the FTIR spectrum of E2 bound NIP submicron particles, the -OH stretching vibration peak has shifted (from the  $3436.7\text{ cm}^{-1}$  for NIP submicron particles before E2 binding) to a lower wavenumber of  $3423.7\text{ cm}^{-1}$  after binding. To confirm this -OH stretching vibration shift phenomenon, spectrum (c) was measured for a mixture of NIP submicron particles and E2 particles. The -OH stretching vibration peak is observed at  $3439.7\text{ cm}^{-1}$  which is very close to that for NIP submicron particles (before E2 binding) at  $3436.7\text{ cm}^{-1}$ . As no hydrogen bonding can occur between NIP submicron particles and E2 particles, the -OH stretching vibration peak is expected to undergo very limited shift. In general, the spectrum (b) of E2 bound NIP submicron particles shows a C=O peak (which belongs to the NIP submicron particles) at a wavenumber of  $1730.4\text{ cm}^{-1}$  and a couple of aromatic C=C peaks (which belong to E2) between wave numbers  $1610.4$  to  $1451.5\text{ cm}^{-1}$ .

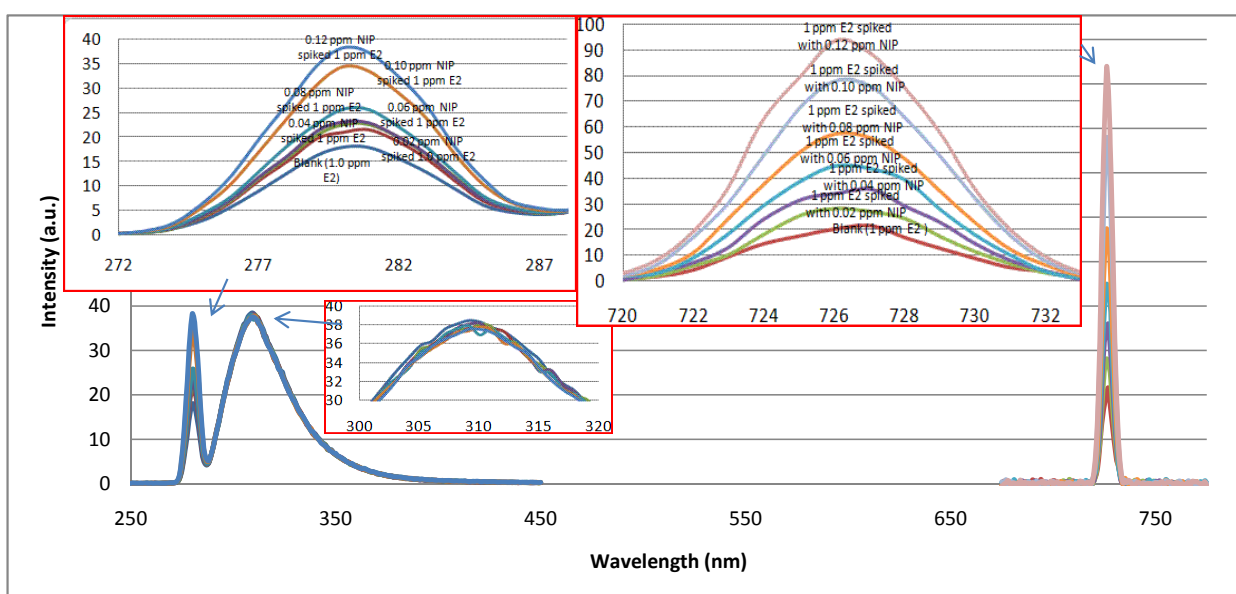
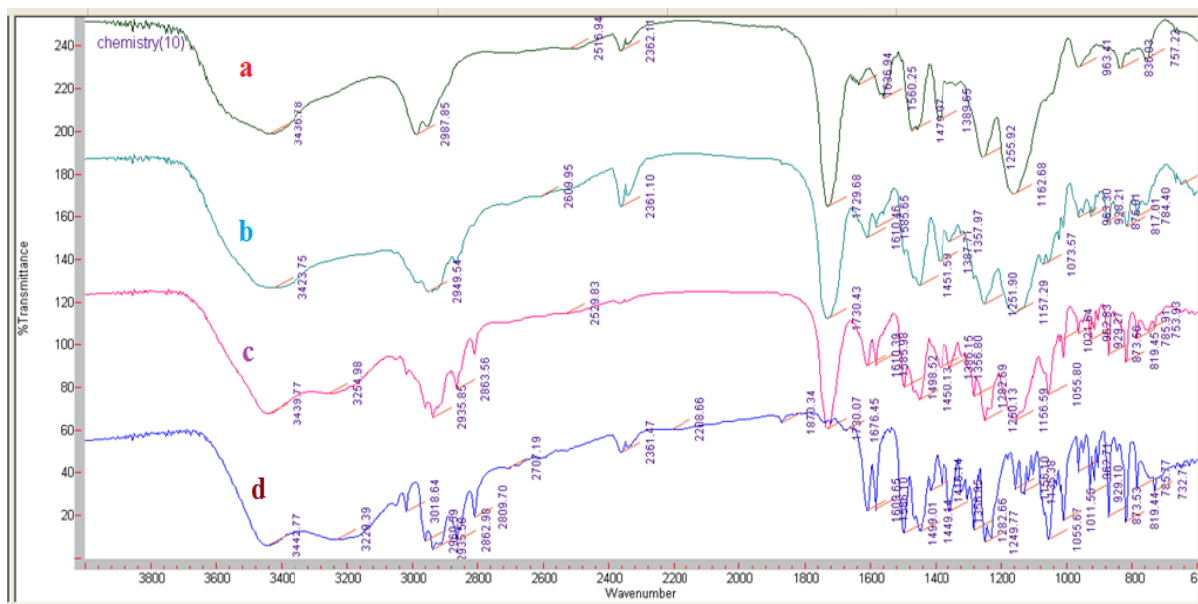


Fig. (7). Fluorescence emission and light scattering spectra of 1.0-ppm E2 aqueous solution spiked with various concentrations of NIP submicron particles, using excitation wavelengths of  $279\pm 1$  nm and  $725\pm 1$  nm.



**Fig. (8).** FTIR spectra of (a) poly MAA-co-EGDMA particles before E2 binding, (b) poly MAA-co-EGDMA particles after binding with E2, (c) poly MAA-co-EGDMA and E2 particles in mixture, and (d) E2 particles.

#### 4. CONCLUSIONS

Mie scattering of PMAA-co-EGDMA non-imprinted polymer submicron particles ( $300 \pm 5$  nm) in aqueous suspension has been studied systematically using various excitation wavelengths from 200 nm to 750 nm. The optimal excitation wavelength was  $725 \pm 1$  nm, which provided a sharp peak with the highest intensity for sensitive determination of NIPs in aqueous suspension. The light scattering peak also allowed accurate determination of trace E2 (as low as 0.1 ppm) in water samples spiked with NIP particles. This new E2 determination method can be attributed to binding between E2 molecules and NIP particles, as characterized by using FTIR spectroscopy. It is also applicable for the determination of bisphenol A (BPA) which is not naturally fluorescent. 700-750 nm is truly an optimal wavelength range for light scattering measurements because laser diodes of high power are commercially available at a reasonable price. NIP submicron particles have one more advantage of being optically transparent (at least translucent). As such, binding of organic contaminants with these particles will allow on-line spectroscopic monitoring by molecular fluorescence and possibly UV-visible spectrophotometry. This is of great importance because the absorbance value and emission intensity can readily indicate when the particles are saturated with contaminants and hence should be regenerated. Automation of these two steps, monitoring and regeneration, are in principle easy to implement from the engineer's perspective for water treatment applications.

Further investigation will be performed by measuring fluorescence emission and light scattering intensities from molecular imprinted polymer (MIP) submicron particles, before and after binding with E2. MIP particles have a porous structure which can do more specific and semi-specific binding with E2 than NIPs. One big challenge is that the fluorescence emission and light scattering from E2 molecules bound inside the cavities can be changed (in intensity

and wavelengths) by MIPs porous structure. Future study will examine spectroscopically the mechanisms of competitive binding of E1/E2/EE2/E3 mixture to MIP submicron particles, as previously proposed in the framework of the NICA-Donnan model [27]. The evolution of time-resolved laser-induced fluorescence spectra of MIP with bound E2, for instance, could show two strikingly different environments for the binding. Release into the bulk solution as free E2 could be evidenced both by the shapes of the spectra and by the decrease in the luminescence decay times.

#### ACKNOWLEDGMENT

Financial support of the Natural Sciences and Engineering Research Council (NSERC) Canada is gratefully acknowledged.

#### REFERENCES

- [1] Pichon, V.; Chapuis-Hugon, F. Role of molecularly imprinted polymers for selective determination of environmental pollutants—A review. *Anal. Chim. Acta*, **2008**, *622*, 48-61.
- [2] Le Noir, M.; Plieva, F.; Hey, T.; Guieysse, B.; Mattiasson, B. Macroporous molecularly imprinted polymeryogel composite systems for the removal of endocrine disrupting trace contaminants. *J. Chromatogr. A*, **2007**, *1154*, 158-164.
- [3] Sanchez-Barragan, I.; Karim, K.; Costa-Fernandez, J.M.; Piletsky, S.A.; Sanz-Medel, A. A molecularly imprinted polymer for carbaryl determination in water. *Sens. Actuat: B Chem.*, **2007**, *123*, 798-804.
- [4] Wei, Y.; Qiu, L.; Yu, J.C.C.; Lai, E.P.C. Molecularly imprinted solid phase extraction in a syringe needle packed with Polypyrrole-encapsulated carbon nanotubes for determination of Ochratoxin A in Red Wine. *Food Sci. Tech.*, **2007**, *13*, 375-380.
- [5] Zhang, Z.; Hu, J. Selective removal of estrogenic compounds by molecular imprinted polymer (MIP). *Water Res.*, **2008**, *42*, 4101-4108.
- [6] Caro, E.; Marce, R.M.; Cormack, P.A.G.; Sherrington, D.C.; Borrull, F. On-line solid-phase extraction with molecularly imprinted polymers to selectively extract substituted 4-chlorophenols and 4-nitrophenol from water. *J. Chromatogr. A*, **2003**, *995*, 233-238.

- [7] Le Moullec, S.; Truong, L.; Montauban, C.; Begos, A.; Pichon, V.; Bellier, B. Extraction of alkyl methylphosphonic acids from aqueous samples using a conventional polymeric solid-phase extraction sorbent and a molecularly imprinted polymer. *J. Chromatogr. A*, **2007**, *1139*, 171-177.
- [8] Michailof, C.; Manesiotis, P.; Panayiotou, C. Synthesis of caffeic acid and p-hydroxybenzoic acid molecularly imprinted polymers and their application for the selective extraction of polyphenols from olive mill waste waters. *J. Chromatogr. A*, **2008**, *1182*, 25-33.
- [9] Da Costa Silva, R.G.; Augusto, F. Sol-gel molecular imprinted ormosil for solid-phase extraction of methylxanthines. *J. Chromatogr. A*, **2006**, *1114*, 216-223.
- [10] Harvey, S.D. Molecularly imprinted polymers for selective analysis of chemical warfare surrogate and nuclear signature compounds in complex matrices. *J. Sep. Sci.*, **2005**, *28*, 1221-1230.
- [11] Beltran, A.; Caro, E.; Marce, R.M.; Cormack, P.A.G.; Sherrington, D.C.; Borrull, F. Synthesis and application of a carbamazepine-imprinted polymer for solid-phase extraction from urine and wastewater. *Anal. Chim. Acta*, **2007**, *597*, 6-11.
- [12] Benito-Pena, E.; Urraca, J.L.; Sellergren, B.; Moreno-Bondi, M.C. Solid-phase extraction of fluoroquinolones from aqueous samples using a water-compatible stoichiometrically imprinted polymer. *J. Chromatogr. A*, **2008**, *1208*, 62-70.
- [13] Horiguchi, H.; Takiguchi, N.; Cho, H. S.; Kojima, M.; Kaya, M.; Shiraishi, H.; Morita, M.; Hirose, H.; Shimizu, M. Ovo-testis and disturbed reproductive cycle in the giant abalone, *Haliotis madaka*: possible linkage with organotin contamination in a site of population decline. *Mar. Environ. Res.*, **2000**, *50*, 223-229.
- [14] Depledge, M.H.; Billingham, Z. Ecological significance of endocrine disruption in marine invertebrates. *Mar. Pollut. Bull.*, **1999**, *39*, 32-38.
- [15] Birnbaum, L.S. Developmental effects of dioxins and related endocrine disrupting chemicals. *Toxicol. Lett.*, **1995**, *82*, 743-750.
- [16] Wuttke, W.; Jarry, H.; Seidlova, D. Endocrine disrupters. *Reproduktionsmedizin*, **1999**, *15*, 173-178.
- [17] Golden, R.J.; Noller, K.L.; Titus-Ernstoff, L.; Kaufman, R.H.; Mittendorf, R.; Stillman, R.; Reese, E.A. Environmental endocrine modulators and human health: an assessment of the biological evidence. *Crit. Rev. Toxicol.*, **1998**, *28*, 109-227.
- [18] Noir, M.L.; Lepeuple, A.S.; Guieysse, B.; Mattiasson, B. Selective removal of 17 $\beta$ -estradiol at trace concentration using a molecularly imprinted polymer. *Water Res.*, **2007**, *41*, 2825-2831.
- [19] Zhu, Q.; Wang, L.; Wu, S.; Joseph, W.; Gu, X.; Tang, J. Selectivity of molecularly imprinted solid phase extraction for sterol compounds. *Food Chem.*, **2009**, *113*, 608-615.
- [20] Watabe, Y.; Kubo, T.; Nishikawa, T.; Fujita, T.; Kaya, K.; Hosoya, K. Fully automated liquid chromatography-mass spectrometry determination of 17 $\beta$ -estradiol in river water. *J. Chromatogr. A*, **2006**, *1120*, 252-259.
- [21] Rachkov, A.; McNiven, S.; El'skaya, A.; Yano, K.; Karube, I. Fluorescence detection of  $\beta$ -estradiol using a molecularly imprinted polymer. *Anal. Chim. Acta*, **2000**, *405*, 23-29.
- [22] Wei, S.; Molinelli, A.; Mizaikoff, B. Molecularly imprinted micro and nanospheres for the selective recognition of 17 $\beta$ -estradiol. *Bio-sens. Bioelectron.*, **2006**, *21*, 1943-1951.
- [23] Horvath, H. Gustav Mie and the scattering and absorption of light by particles: Historic developments and basics. *J. Quant. Spectrosc. Radiat. Transf.*, **2009**, *110*, 787-799.
- [24] Gendrin, C.; Roggo, Y.; Collet, C. Pharmaceutical applications of vibrational chemical imaging and chemometrics: a review. *J. Pharm. B.*, **2008**, *48*, 533-553.
- [25] Costello, M.J.; Johnsen, S.; Gilliland, K.O.; Freel, C.D.; Fowler, W.C. Predicted light scattering from particles observed in human age-related nuclear cataracts using mie scattering theory. *Invest. Ophthalmol. Vis. Sci.*, **2007**, *48*, 303-312.
- [26] Cai, W.; Ma, L. Information content of scattering measurements and characterization of spheroids. *J. Aerosol Sci.*, **2008**, *39*, 1032-1039.
- [27] Marang, L.; Eidner, S.; Kumke, M.U.; Benedetti M.F.; Reiller, P.E. Spectroscopic characterization of the competitive binding of Eu(III), Ca(II), and Cu(II) to a sedimentary originated humic acid. *Chem. Geol.*, **2009**, *264*, 154-161.

Received: August 14, 2009

Revised: October 21, 2009

Accepted: October 21, 2009

© Yang et al.; Licensee Bentham Open.

This is an open access article licensed under the terms of the Creative Commons Attribution Non-Commercial License (<http://creativecommons.org/licenses/by-nc/3.0/>) which permits unrestricted, non-commercial use, distribution and reproduction in any medium, provided the work is properly cited.